Tonic GABAA Conductance Bidirectionally Controls Interneuron Firing Pattern and Synchronization in the CA3 Hippocampal Network

Ivan Pavlov[a,1,2], Leonid P. Savtchenko[a,b,1], Inseon Song[b,1], Jaeyeon Koo[b], Alexey Pimashkin[c], Dmitri A. Rusakov[a,2], Alexey Semyanov[b,c,2]

[1]Contributed equally to this work. [2]To whom correspondence may be addressed. E-mail: semyanov@brain.riken.jp, or i.pavlov@ucl.ac.uk, or d.rusakov@ucl.ac.uk [a]UCL Institute of Neurology, London, Great Britain [b]RIKEN Brain Science Institute, Wako-shi, Saitama, Japan [c]University of Nizhny Novgorod, Nizhny Novgorod, Russia

Submitted to Proceedings of the National Academy of Sciences of the United States of America

The spiking output of interneurons is key for rhythm generation in the brain. However, what controls interneuronal firing remains incompletely understood. Here we combine dynamic-clamp experiments with neural network simulations to understand how tonic GABAA conductance regulates the firing pattern of CA3 interneurons. In baseline conditions tonic GABAA depolarizes these cells, thus exerting an excitatory action while also reducing the EPSP amplitude through shunting. As a result, the emergence of weak tonic GABAA conductance transforms the interneuron firing pattern driven by individual EPSPs into a more regular spiking mode determined by the cell intrinsic properties. The increased regularity of spiking parallels stronger synchronization of the local network. With further increases in tonic GABAA conductance the shunting inhibition starts to dominate over excitatory actions and thus moderates interneuronal firing. The remaining spikes tend to follow the timing of suprathreshold EPSPs and thus become less regular again. The latter parallels a weakening in network synchronization. Thus, our observations suggest that tonic GABAA conductance can bidirectionally control brain rhythms through changes in the excitability of interneurons and in the temporal structure of their firing patterns.

tonic conductance | extrasynaptic signaling | GABA | brain rhythm | interneurons

Rhythmic activity paces signal transfer within brain circuits. Brain rhythms are believed to depend heavily on the networks of inhibitory interneurons (1-4). In addition to synaptic inputs, interneuron excitability in the hippocampus is determined by tonic $GABA_A$ conductance (5, 6), which could thus contribute to hippocampal rhythmogenesis. Indeed, GABA transaminase inhibitor vigabatrin increases the ambient GABA concentration, enhancing the power of the theta-rhythm in rats (7). In mice expressing GFP under the GAD67 promoter the reduced levels of ambient GABA correlate with a decreased power of kainate-induced oscillations *in vitro* (8). The latter decrease is reversed by a GABA uptake inhibitor, guvacine, which raises ambient GABA. GABA release by astrocytes also increases the gamma oscillation power in hippocampal area CA1 *in vivo* (9). Intriguingly, in hippocampal slices of animals lacking δ subunit-containing $GABA_A$ receptors (which mediate tonic conductance in many local cell types including interneurons) the average frequency of cholinergically-induced gamma oscillations is increased whereas the oscillation power tends to drop (10). However, cellular mechanisms underlying such phenomena remain poorly understood.

One possible explanation is the influence of tonic $GABA_A$ conductance on the firing pattern of interneurons. Activation of $GABA_A$ receptors inhibits most neurons, through either membrane hyperpolarization or shunting, or both (11). In the adult brain, a depolarizing action of GABA has also been reported in various cell types, including hippocampal interneurons (3, 12-15). GABAergic depolarization can prompt spike generation, thus countering the shunting effects (14, 16). Therefore, experimental evidence indicates that the net effect of $GABA_A$ receptor activation combines the excitatory action of depolarization and the inhibitory consequences of shunting, with the latter prevailing when the $GABA_A$ receptor conductance is sufficiently strong. As a result, increasing the tonic $GABA_A$ signaling can have a biphasic effect on individual hippocampal interneurons: excitatory at weak conductances and inhibitory at strong (14). Here we find that weak tonic $GABA_A$ conductance favors a more regular firing pattern of interneurons thus facilitating synchronization of the CA3 network. In contrast, strong $GABA_A$ conductance makes the firing pattern more dependent on the stochastic excitatory synaptic input, thus reducing network synchrony.

Results

Varied tonic $GABA_A$ conductance regulates interneuron firing pattern

In acute hippocampal slices, we recorded from visually identified, fast-spiking CA3 *stratum lucidum* interneurons (which displayed relatively heterogeneous morphologies, Fig. S1A) (17). AMPA, NMDA and $GABA_B$ receptors were pharmacologically blocked throughout. In perforated-patch mode, E_{GABA} was above the resting membrane potential (RMP = -71.0 ± 1.5 mV; E_{GABA} = -64.3 ± 2.5 mV; $n = 5$, $P = 0.013$ paired t-test; Fig. 1A) (3, 12,

Significance

We demonstrate a novel property of interneuron physiology that has a major implication for understanding how rhythmic activity in the brain is so seamlessly generated from normal spiking. The property we describe is the graded response of the tonic $GABA_A$ conductance in interneurons. We find that, as this interneuron conductance transitions from low to high levels, it fundamentally changes the input mode for interneuron firing from being a faithful readout for external firing to becoming attuned to intrinsic firing properties. It is the latter mode that supports oscillations in brain networks. Our discovery provides the missing mechanism underlying the switch in firing modes and resolves a major controversy on the functional role of tonic GABA in the control of firing.

Reserved for Publication Footnotes

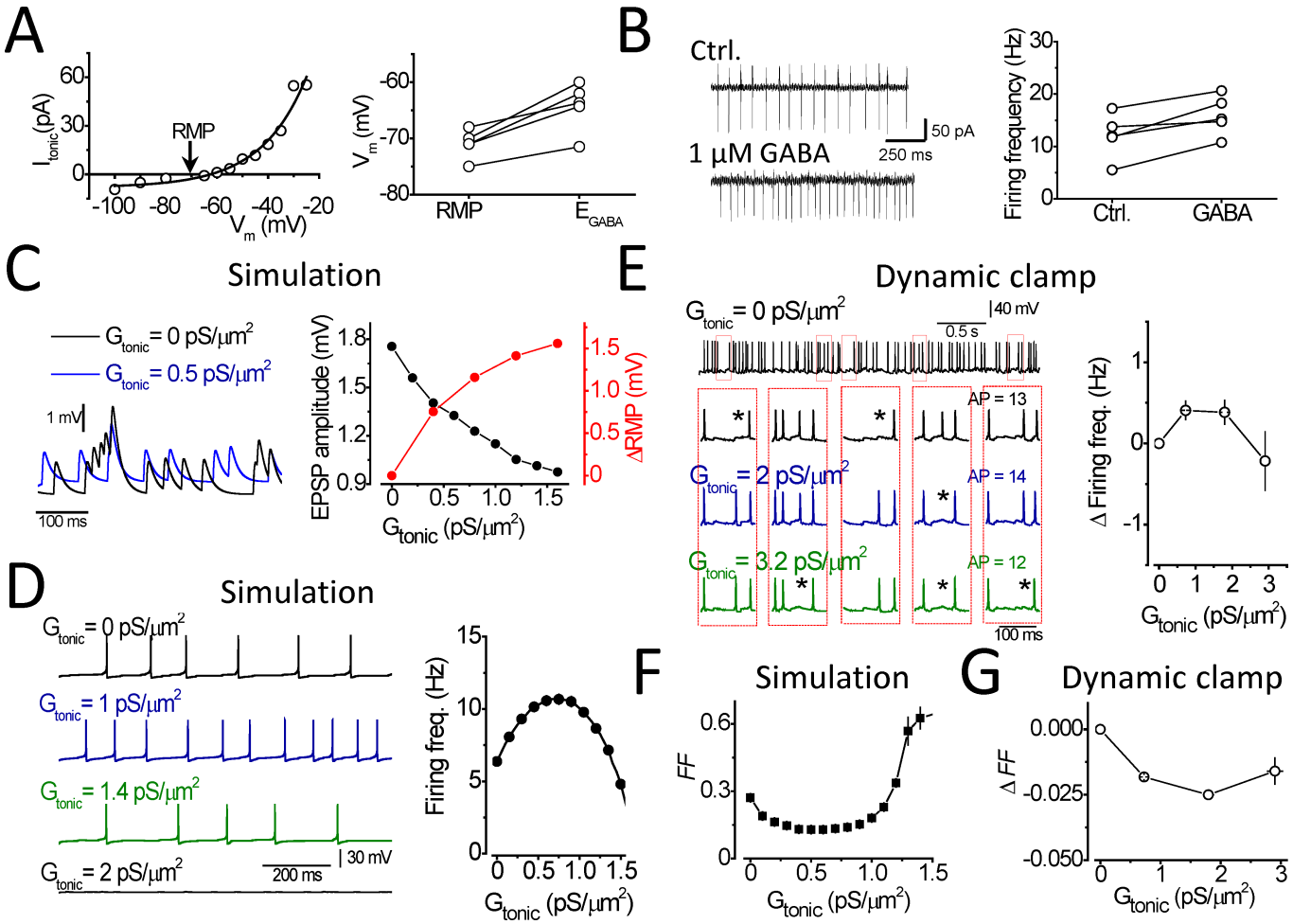

Fig. 1. The effect of G_{tonic} on electrical activity of an interneuron. (A) Reversal potential of tonic $GABA_A$ current (E_{GABA}) in CA3 interneurons. *Top*, current-voltage relationship of the tonic $GABA_A$-mediated current (I_{tonic}; perforated-patch). Black, second-order polynomial fit. E_{GABA} is an intercept of membrane voltage (V_m) axis and the fit; arrow, RMP. *Bottom*, RMP and E_{GABA} in 5 individual cells. (B) The effect of 1 μM GABA on spontaneous firing in CA3 interneurons. *Top*, sample traces; *Bottom*, spontaneous firing frequencies (5 cells in control and in 1 μM GABA). (C) *Left*, simulated EPSPs with and without G_{tonic}. *Right*, mean EPSP amplitude (black; G_{Na} = 0 pS/μm^2) and a change in the resting V_m (ΔRMP) plotted against G_{tonic} (red). (D) *Left*, simulated APs induced by random EPSPs at three different values of G_{tonic}. *Right*, mean firing frequency of a model cell against G_{tonic}; solid line, second order polynomial fit. (E) *Left*, Sample traces showing firing of an interneuron in response to a Poisson process of excitatory synaptic conductances injected using dynamic clamp. Boxes, 5 zoomed parts of the trace at three different values of G_{tonic}. Asterisks, missing APs. AP number, total AP number in the boxed areas for each G_{tonic}. *Right*, mean firing frequency against G_{tonic} (n = 14). (F) and (G) Fano factor (*FF*) plotted against G_{tonic} in the modelled interneuron (F) and in dynamically-clamped interneurons (G, n = 14). Error bars, SEM.

13), and 1 μM GABA added to the bath increased spontaneous firing of interneurons (cell-attached mode, Fig. 1B). In these experiments, excitatory transmission was blocked to isolate the effect of tonic $GABA_A$ conductance (G_{tonic}). However, interneurons in vivo undergo depolarization by the excitatory postsynaptic potentials (EPSPs), which could, in principle, counteract or even reverse the effect of G_{tonic}. To test the biophysical plausibility of this hypothesis we explored a single-compartment model of an interneuron (Methods). First we examined the relationship between G_{tonic} and the waveform of randomly generated EPSPs (averaged frequency = 20 Hz; peak synaptic conductance, G_s = 0.4 nS) in a non-spiking cell (Na^+ channels omitted). We found that increasing G_{tonic} depolarized the cell while decreasing the EPSP amplitude (Fig. 1C), thus transforming the phasic, fluctuating excitatory input into smoother, tonic excitation. Next, we repeated these simulations in a spiking interneuron (voltage-dependent Na^+ channels, G_{Na} = 350 pS/μm^2) and found a biphasic, bell-shaped effect on the cell firing rate (Table S1; Fig. 1D) similar to that reported in CA1 interneurons in the absence of the glutamatergic excitatory input (14).

To test these theoretical predictions we used dynamic-clamp experiments. First, we established the cell firing threshold, by injecting excitatory postsynaptic conductance waveforms (EPSG) of varying magnitudes, and set the E_{GABA} at the identified threshold value. Next, were simulated EPSPs by applying randomly generated EPSGs (mean frequency 60 Hz). APs were thus triggered stochastically when EPSP summation exceeded the threshold (mean AP frequency: 12.33 ± 0.86 Hz). Elevation of G_{tonic} produced a biphasic change in the CA3 interneuron firing rate (Table S1; Fig. 1E). (The quantitative difference in the effect's sensitivity to G_{tonic} between modeled and dynamically-clamped interneurons was likely due to an additional shunting influence of dendrites in real neurons.)

We next simulated the effect of G_{tonic} on interneuron firing under stochastic EPSG input. When cells are excited by relatively sparse random EPSPs, the resulting AP firing tends to follow their random pattern. However, when cells are excited by sustained depolarization their firing depends mainly on the intrinsic cell properties and thus tends to be more regular. Because weak G_{tonic} excites interneurons while reducing the EPSP amplitude

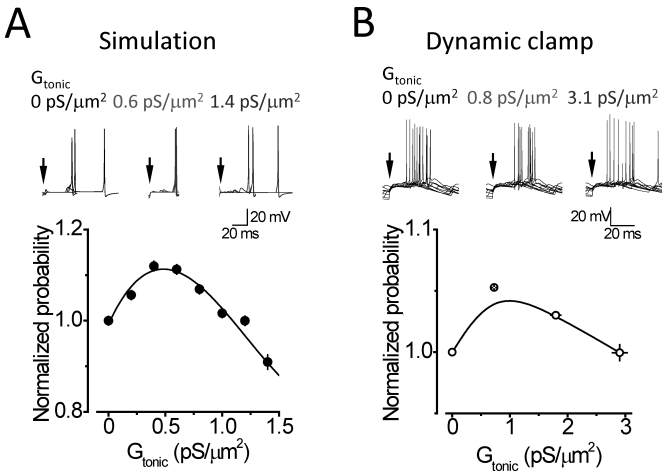

Fig. 2. G_{tonic} biphasically regulates probability of post-IPSG spiking. (A) and (B) Spiking probability within 80 ms (A) and 45 ms (Bpost-IPSG in the modelled interneuron (A) and in the dynamic-clamp experiment (B; n = 14). Upper panels, superimposed traces showing the first post-IPSG spike; arrow, IPSG onset. Graphs, AP probability post-IPSG versus G_{tonic}; values normalized to control (G_{tonic} = 0 pS/µm^2); data points are fit with the polynomial function; error bars, SEM.

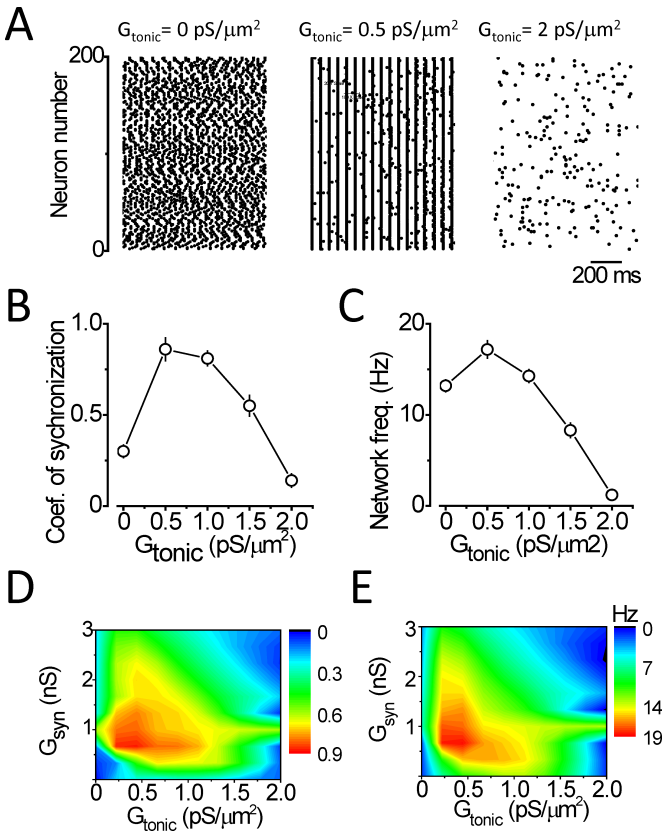

Fig. 3. Synchronization of the interneuronal network depends on G_{tonic}. (A) Raster plot of spike times for each interneuron in the simulated network at three values of G_{tonic} (0, 0.5 and 2 pS/µm^2). (B) and (C) Mean network synchronization (B) and frequency (C) versus G_{tonic}. (D) and (E) Color diagrams, network synchronization (D) and frequency (E) versus G_{syn} and G_{tonic}; error bars, SEM.

(see above), we hypothesized that it should make their firing more regular. In contrast, strong G_{tonic} lowers cell excitability through shunting, and therefore cell spiking should be driven

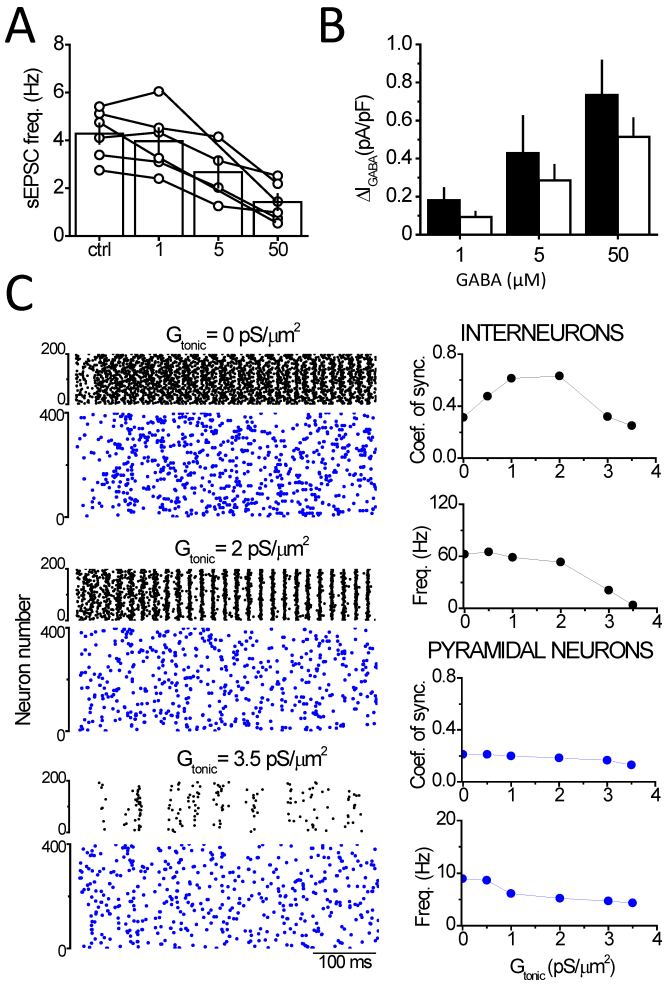

Fig. 4. Effects of G_{tonic} on the network behavior. (A) The effect of ambient GABA on the frequency of spontaneous EPSPs (sEPSPs) in CA3 interneurons; error bars, SEM. (B) Tonic current density in CA3 interneurons and pyramidal neurons versus GABA concentration (black, interneurons; open, pyramids); error bars, SEM. (C) Computer simulated effects of G_{tonic} on the spiking frequency and synchronization in a model with a feedback between interneurons and pyramidal neurons. *Left*, raster plots of spike times versus G_{tonic}; black, interneurons; blue, pyramidas; panels show first 500 ms. *Right*, graphs, the coefficient of synchronization and firing frequency in interneurons and pyramidal cells versus G_{tonic}; G_{tonic} values shown; G_{tonic} in pyramidal cells were set twice smaller to reflect the difference in the tonic current density.

by EPSPs exceeding the threshold. We tested this prediction by calculating the Fano factor (*FF*) (18), a statistical indicator of randomness ranging from 1 (random) to 0 (regular), for inter-spike intervals documented in the above simulations and in the *in situ* experiments. Indeed, weak G_{tonic} decreased the *FF* while strong G_{tonic} increased it, both in the model cell and in the CA3 interneurons which received random excitatory input (Table 1; Fig. 1 F,G). In striking contrast, when the model cell received constant excitatory conductance instead of EPSGs, its firing pattern remained regular (*FF* = 0), regardless of G_{tonic} magnitude (Fig. S2). In these conditions an excitatory effect of weak G_{tonic} on the cell firing frequency was small, while strong G_{tonic} still had a profound inhibitory action.

Tonic $GABA_A$ conductance biphasically regulates spike occurrence in the pre-synchronized network in vitro

Interconnected interneurons synchronize their activity through mutual inhibition during their concurrent spiking (3, 19). The latter produces shunting IPSGs which prevent firing

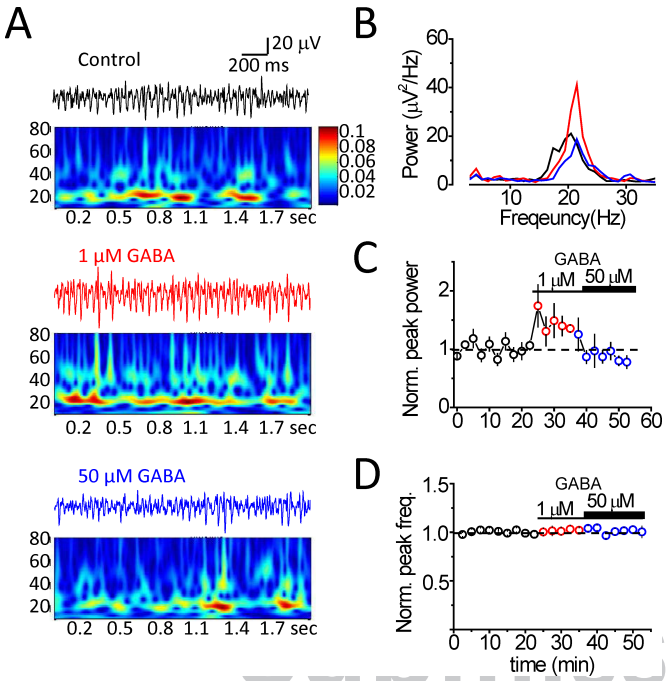

Fig. 5. . Ambient GABA biphasically regulates carbachol-induced oscillations of the LFP. (A) Sample traces of the LFP and corresponding wavelet transforms in control, in the presence of 1 μM GABA (*red trace*) and 50 μM GABA (*blue trace*). (B) Power spectral density of oscillations in control (*black trace*), 1 μM GABA (*red trace*) and 50 μM GABA (*blue trace*) (C) and (D) time course of normalized peak magnitude (C) and peak frequency (D) of power spectral density in control and during subsequent applications of 1 μM GABA and 50 μM GABA.

of postsynaptic interneurons; this can be shown experimentally using IPSGs evoked by extracellular stimulation (Fig. S3A). Coordinated firing of interneurons released from mutual inhibition produces another round of mutual inhibition, the cycle which could eventually synchronize the network. The more interneurons contribute to the mutual inhibition the stronger is the synchronization. We used this phenomenon to test the effect of G_{tonic} on network synchronies, by recording the probability of spiking within a fixed time interval after an evoked IPSG (5-50 ms post-IPSG in simulations and 5-85 ms in dynamic-clamp experiments; Methods). Weak G_{tonic} increased this probability both in the model cell (to 111.2 ± 0. 001 % of control at G_{tonic} = 0.6 pS/μm^2, n = 50000 simulation runs, $P < 0.001$, paired t-test; Fig 2A) and in dynamically-clamped interneurons (to 105.2 ± 0.01 % of control at G_{tonic} = 0.73 ± 0.03 pS/μm^2, n = 14, $P < 0.001$, paired t-test; Fig. 2B). Strong G_{tonic} decreased the probability of post-IPSG spiking (model cell: to 90 ± 0.0001 % of control at G_{tonic} = 1.4 pS/μm^2, n = 50000 simulation runs, $P <$ 0.001, paired t-test; dynamic clamp: to 99 ± 0.06 % of control at G_{tonic} = 2.9 ± 0.12 pS/μm^2, n = 14, $P = 0.9$, paired t-test).

Changes in the post-IPSG spike probability can reflect changes in the firing frequency, or pattern, or both. To discern between these possibilities, we explored effects of G_{tonic} in conditions of regular firing, under sustained depolarizing conductance. Varying G_{tonic} altered the firing frequency but not the post-IPSG spike probability (until the firing became so infrequent that APs failed to appear in the sampling window post-IPSG; Fig. S3B). This result points to the firing pattern as the main factor in regulating post-IPSG spike probability. Indeed, the first post-IPSG spike is generated when depolarization reaches the threshold: under constant excitation this will depend mainly on the IPSG decay time course. In contrast, under synaptic excitation an important trigger will be the arrival of a suprathreshold EPSP.

Tonic $GABA_A$ conductance biphasically regulates synchronization of simulated interneuronal networks

To understand how above phenomena translate into the network synchronization properties we explored a simulated network of 200 interconnected interneurons (3) (Methods). In agreement with a previous report (3), excitatory drive consisting of Poisson-process EPSPs produced weaker synchronization (coefficient of synchronization, CS: 0.3 ± 0.035; network frequency 13.2 ± 0.66 Hz, n = 10; Fig. 3A,B) compared to sustained excitation (CS: 0.8 ± 0.063 Hz, n = 10; difference at $P < 0.001$; Fig. S4). Weak G_{tonic} (0.5 pS/μm^2) increased network synchronization (CS: 0.86 ± 0.063, n = 10, $P < 0.001$ for difference with G_{tonic} = 0; Fig. 3 A,B) and frequency (17.18 ± 0.959 Hz, n = 10, $P < 0.001$; Fig. 3 A,C). Further elevating G_{tonic} decreased these parameters (at G_{tonic} = 2.0 pS/μm^2 CS: 0.14 ± 0.037, n = 10, $P < 0.001$ for difference with G_{tonic} = 0; frequency: 1.2 ± 0.56 Hz; n = 10, $P <$ 0.001; Fig. 3 A-C). When interneurons were excited by constant depolarization, increasing G_{tonic} reduced both synchronization and frequency monotonically (Fig. S4), suggesting that the action of G_{tonic} depends on the mode of excitation.

Another important factor which can alter the effects of G_{tonic} on network synchronization and frequency is the connection strength among interneurons (unitary synaptic conductance, G_{syn}) (3). Indeed, when G_{syn} was at its low or high limit G_{tonic} failed to synchronize the network (Fig. 3D). Nevertheless, the synchronizing effects of G_{tonic} were observed within a wide range of physiological G_{syn} (0.4 - 2.4 nS). Similar effects were seen for the network frequency (Fig. 3E). Thus G_{syn} determines the range within which G_{tonic} enhanced synchronization and increased the network frequency.

In contrast to the above simplified model, real neural networks in the CA3 area feature a feedback from interneurons to pyramidal neurons (2, 20). In adult pyramidal cells, however, the E_{GABA} is hyperpolarizing (17), and thus tonic $GABA_A$ conductance exerts a purely inhibitory action. Indeed, bath application of GABA robustly reduces the frequency of spontaneous excitatory post-synaptic currents (sEPSCs) in interneurons (Fig. 4A). Because this effect might in principle affect the ability of G_{tonic} to regulate synchronization of interneurons, we tested its consequences by incorporating connections between interneurons and pyramidal neurons in the CA3 network model (*SI Text*). G_{tonic} in pyramidal neurons was set at a lower level compared to interneurons, in accordance with the experimental observations (Fig. 4B). Simulations indicated that increasing G_{tonic} in both cell types reduced the firing frequency and synchronization of pyramidal neurons. Nevertheless, similar to the interneuron-only model, we observed a robust biphasic effect of G_{tonic} on synchronization of interneurons (Fig. 4C). In contrast, the interneuron firing frequency was relatively stable within the wide range of G_{tonic}, which is likely due to the dual (excitatory and inhibitory) action of G_{tonic} on the two neuronal populations in the network.

Tonic $GABA_A$ conductance biphasically regulates network synchronization in hippocampal slices

We recorded oscillations of local field potentials (LFP) in the hippocampal CA3 region using 20 μM carbachol with $GABA_B$ receptors blocked. 1 μM GABA increased the power spectrum density peak of LFP oscillations (150.4 ± 16.4 % of control, n = 6, P = 0.024; Fig. 5A-C) whereas subsequent application of 50 μM GABA decreased it (81.4 ± 6.8 % of control, n = 7, P = 0.045). At the same time, GABA applications had little effect no the frequency of carbachol-induced oscillations (Fig. 5D). These observations were fully consistent with our model predictions. To test whether bath applied GABA affects $GABA_A$ receptor-mediated synaptic transmission we compared miniature IPSCs (mIPSCs) in interneurons recorded in control conditions

and after GABA application (50 μM). Similar to area CA1 data (14), GABA had no significant effect on the amplitude (control: 47.9 ± 5.9 pA; GABA: 52.8 ± 7.4 pA; n = 6, p = 0.13) or frequency (control: 4.9 ± 0.2 Hz; GABA: 4.0 ± 0.6 Hz; n = 6, p = 0.19) of mIPSCs. This result indicates that GABA application in our experiments had no significant effect on either postsynaptic $GABA_A$ receptors or presynaptic GABA release.

Discussion

Firing patterns of neurons are crucial for information coding in the brain (21). To enable the full spectrum of spiking sequences, neurons can dynamically shift between the firing mode set by external synaptic input and that reliant mainly on the cell intrinsic properties. The origin of the shift is largely unknown, and our present results suggest that depolarizing G_{tonic} could be its important contributor in hippocampal CA3 interneurons. We have found that weak G_{tonic} not only increases the firing frequency in these cells, but also changes their firing mode. When interneurons are excited by the randomly occurring, relatively sparse EPSPs, the cells generally follow this EPSP time series. Such 'EPSP-driven' firing does not favor synchronization of interneuron networks. Weak G_{tonic} depolarizes interneurons, but at the same time shunts EPSPs, thus converting a phasic synaptic input sequence into more tonic excitation. In these conditions the firing becomes more dependent on the intrinsic properties of postsynaptic cells, rather than on the excitatory synaptic input, favoring a more regular, 'deterministic' mode. Regular interneuron firing enhances synchronization in the network and therefore promotes rhythmic activity. In contrast, strong G_{tonic} shifts the firing of interneurons back to the input-driven, 'probabilistic' mode, thus weakening network synchronization.

The present results suggest that tonic inhibition affects synchrony or power, rather than the frequency, of network oscillations whereas a previous report found an inverse association of tonic conductance with the oscillation frequency, rather than power (10). However, the earlier work employed genetic deletion of the delta subunit-containing $GABA_A$ receptors as a tool to manipulate tonic conductance, which might subtly shift the network excitability away from the biphasic mode. Indeed, the authors also found what seems to be a large (albeit not statistically validated) decrease in the peak power of oscillations for delta-knockouts (10), which would appear in line with our main conclusion relating low G_{tonic} to facilitated oscillations.

In hippocampal interneurons, the mechanism of post-inhibition (post-IPSG) firing appears to differ from the classical 'rebound' spiking in pyramidal cells, which relies on the hyperpolarization-activated cationic current (*h*-current) following GABA-mediated hyperpolarization (22, 23). The latter mechanism, however, does not operate when E_{GABA} is above the resting membrane potential: indeed, our data indicate that tonic $GABA_A$ conductance affects the probability of post-IPSG spiking in a biphasic manner. Noteworthy, the effect of ambient GABA on the network oscillations is not limited to interneurons. We observed no significant changes in the oscillation frequency produced by exogenous GABA in hippocampal slices thus suggesting an effect pertinent to principal cells. Our simulations incorporating connections between interneurons and pyramidal cells indeed indicate that a decrease in the frequency of pyramidal cell firing may compensate for the biphasic GABA effect on interneuron excitability. Intriguingly, our predictions are consistent with a recently reported effect of increased ambient GABA on gamma oscillations *in vivo,* in which the gamma power was increased without changes in the firing frequency (9) (but see (10)). Assuming that changes in the power of oscillations and in their frequency can have different computation meanings (24), the effect of tonic $GABA_A$ conductance on pyramidal neurons can provide a mechanism enabling increases in the oscillation power without changes in their frequency.

Methods

The methods are briefly described below, for full details see the *SI Text*.

Electrophysiology

Hippocampal slices (350 μm-thick) from 3 to 4-week-old male rats were used for patch-clamp recordings from the CA3 *stratum lucidum* interneurons. Neurons that could sustain firing frequency over 40 Hz were selected for whole-cell and perforated patch recordings. In some experiments interneurons were filled with biocytin (3mg/ml) for reconstruction of their morphology, which indicated that recorded cells belonged to the heterogeneous population (Fig. S1). Whole-cell pipettes for voltage-clamp recordings of tonic $GABA_A$ currents (I_{tonic}) and mIPSCs contained (in mM): 130 CsCl, 8 NaCl, 10 Cs-HEPES, 2 EGTA, 0.2 $MaCl_2$, 2 MgATP, 0.3 Na_2GTP, and 5 QX314Br (pH 7.2, osmolarity 295 mOsm, liquid junction potential 4.1 mV). ΔI_{tonic} was calculated as the difference between the holding current in control and in the presence of exogenous GABA (27). sEPSCs were recorded with solution containing (in mM): 130 Cs-methanesulfonate, 8 NaCl, 10 Na-phosphocreatin, 10 HEPES, 2 EGTA, 2MgATP, 0.4 Na_2GTP, 10 QX314Br (pH 7.2, osmolarity 295 mOsm). Perforated patch recordings were made using KCl-based solution containing 20 μg/ml gramicidin-D. For cell-attached experiments pipettes were filled with the perfusion solution.

In dynamic-clamp experiments excitatory synaptic input was simulated by injecting 5500 ms template consisting of Poisson-distributed EPSGs of constant amplitude (times the unitary conductance of 0.7 nS) and a reversal potential of 0 mV (τ_{rise} = 0.5 ms, τ_{decay} = 5 ms). The amplitude range and mean inter-event interval (16.7 ms) of simulated EPSGs were chosen to evoke cell firing at 10-20 Hz. Large IPSGs representing converging inhibitory input generated by concurrent interneuron firing were simulated by injecting 100 nS $GABA_A$ synaptic conductances (τ_{rise} = 2.5 ms, τ_{decay} = 10 ms). AP threshold of recorded interneurons was estimated by EPSG injections of variable magnitude. E_{GABA} was set in the vicinity of AP threshold (±3 mV).

Oscillations of LFPs were induced by bath application of 20 μM carbachol in horizontal slices placed in the submerged chamber with laminar solution flow above and below the slice (superfusion rate 4-6 ml/min). Recordings were done with glass microelectrodes placed in the CA3 pyramidal layer. $GABA_B$ receptors were blocked throughout experiments.

Simulations: interneuron The model interneuron had a shape of a cylinder (length: 62 μm, diameter: 62 μm; axial resistance: 100 Ohm/cm; C_m: 1μF/cm^2; resting membrane potential: -65 mV) (28). Membrane properties were described using Hodgkin-Huxley formalism (AP threshold $\sim$ -58 mV, determined from the voltage response to a ramp of excitatory current of 1pA/ms). The kinetics of the channels were typical of CA3 hippocampal fast spiking basket cells (3, 21). The model was obtained from ModelDB (https://senselab.med.yale.edu; accession number 21329).

Simulations: neural networks

The interneuron-only network consisted of 200 interconnected cells ($n_{i,i}$ = 1…200) and had a circular architecture. Each cell was connected with 100 other interneurons via GABAergic synapses. Excitatory input was driven by 200 excitatory neurons, each of which independently generated random APs at a rate of 12 Hz. The coefficient of synchronization $k(\tau)$ was calculated as an average value of coefficients $k_{i,j}(\tau)$ for each pair of neurons (*i, j*) in the network. Each coefficient $k_{i,j}(\tau)$ was calculated for intervals of 500 ms. The probability of AP generation after IPSGs was calculated between 5 and 50 ms after the IPSG onset in computer simulations, and between 5 and 85 ms in dynamic clamp experiments. This time-window was chosen so that the AP occurrence after IPSGs decreased approximately *e*-fold.

The interneurons - pyramidal cell network was simulated using a previously reported approach (29) (https://senselab.med.yale.edu; ModelDB accession number 138421). The network consisted of 200 fast spiking interneurons (I) and 400 pyramidal cells (E). I and E cells were modeled as single compartments using the standard Hodgkin-Huxley formulism. The E_{GABA} was set to –57 mV (depolarizing relative to the V_R = –65 mV) in I cells and –72 mV (hyperpolarizing relative to the V_R) in E cells. Neurons had 3 types of connections I – I, I – E and E – I with probabilities set as follows: P_{E-I} = 0.4, P_{I-E} = 0.1 and P_{I-I} = 1.0. E cells were excited by the constant excitatory current. The decay times of synaptic connections were: 10 ms for the I-I IPSGs, 20 ms for the I-E IPSGs, and 4 ms for the E-I EPSGs.

G_{tonic} in computer modeling and dynamic clamp experiments was simulated as previously described to feature experimentally observed outward rectification of tonic currents (30). G_{tonic} values reported in the paper represent maximal values of the voltage-dependent conductance. Computations were carried using an ad hoc built in-house 64-node PC cluster optimized for parallel computing (31).

Statistics

Two-tailed Student's *t*-test (paired or independent as appropriate) was used for the statistical analysis, $P < 0.05$ for significant differences. Data are presented as mean ± SEM.

Acknowledgements .

We thank Drs Hajime Hirase and Iris Oren for their incisive comments. This work was supported by The Wellcome Trust (UK), Epilepsy Research UK, European Research Council and COST Action BM1001, The Royal Society and The Worshipful Company of Pewterers (UK).

1. Mann EO & Paulsen O (2007) Role of GABAergic inhibition in hippocampal network oscillations. Trends Neurosci 30(7):343-349.
2. Bartos M, Vida I, & Jonas P (2007) Synaptic mechanisms of synchronized gamma oscillations in inhibitory interneuron networks. Nat Rev Neurosci 8(1):45-56.
3. Vida I, Bartos M, & Jonas P (2006) Shunting inhibition improves robustness of gamma oscillations in hippocampal interneuron networks by homogenizing firing rates. Neuron 49(1):107-117.
4. Whittington MA, Traub RD, & Jefferys JG (1995) Synchronized oscillations in interneuron networks driven by metabotropic glutamate receptor activation. Nature 373(6515):612-615.
5. Semyanov A, Walker MC, Kullmann DM, & Silver RA (2004) Tonically active GABA A receptors: modulating gain and maintaining the tone. Trends Neurosci 27(5):262-269.
6. Semyanov A, Walker MC, & Kullmann DM (2003) GABA uptake regulates cortical excitability via cell type-specific tonic inhibition. Nat Neurosci 6(5):484-490.
7. Bouwman BM, Heesen E, & van Rijn CM (2004) The interaction between vigabatrin and diazepam on the electroencephalogram during active behaviour in rats: an isobolic analysis. Eur J Pharmacol 495(2-3):119-128.
8. Lu CB, Yanagawa Y, & Henderson Z (2010) Properties of gamma frequency oscillatory activity induced in hippocampal slices from the adult GAD67-GFP (Deltaneo) mouse. Brain Res.
9. Heja L, et al. (2012) Astrocytes convert network excitation to tonic inhibition of neurons. BMC biology 10:26.
10. Mann EO & Mody I (2010) Control of hippocampal gamma oscillation frequency by tonic inhibition and excitation of interneurons. Nat Neurosci 13(2):205-212.
11. Farrant M & Kaila K (2007) The cellular, molecular and ionic basis of GABA(A) receptor signalling. Prog Brain Res 160:59-87.
12. Michelson HB & Wong RK (1991) Excitatory synaptic responses mediated by GABAA receptors in the hippocampus. Science 253(5026):1420-1423.
13. Verheugen JA, Fricker D, & Miles R (1999) Noninvasive measurements of the membrane potential and GABAergic action in hippocampal interneurons. J Neurosci 19(7):2546-2555.
14. Song I, Savtchenko L, & Semyanov A (2011) Tonic excitation or inhibition is set by GABA(A) conductance in hippocampal interneurons. Nat Commun 2:376.
15. Sauer JF, Struber M, & Bartos M (2012) Interneurons provide circuit-specific depolarization and hyperpolarization. J Neurosci 32(12):4224-4229.
16. Zhang SJ & Jackson MB (1995) GABAA receptor activation and the excitability of nerve terminals in the rat posterior pituitary. J Physiol 483 (Pt 3):583-595.
17. Banke TG & McBain CJ (2006) GABAergic input onto CA3 hippocampal interneurons remains shunting throughout development. J Neurosci 26(45):11720-11725.
18. Fano U (1947) Ionization Yield of Radiations .2. The Fluctuations of the Number of Ions. Phys Rev 72(1):26-29.
19. Wang XJ & Buzsaki G (1996) Gamma oscillation by synaptic inhibition in a hippocampal interneuronal network model. J Neurosci 16(20):6402-6413.
20. Fisahn A, Pike FG, Buhl EH, & Paulsen O (1998) Cholinergic induction of network oscillations at 40 Hz in the hippocampus in vitro. Nature 394(6689):186-189.
21. Hopfield JJ (1995) Pattern recognition computation using action potential timing for stimulus representation. Nature 376(6535):33-36.
22. Ascoli GA, Gasparini S, Medinilla V, & Migliore M (2010) Local control of postinhibitory rebound spiking in CA1 pyramidal neuron dendrites. J Neurosci 30(18):6434-6442.
23. Manseau F, Goutagny R, Danik M, & Williams S (2008) The hippocamposeptal pathway generates rhythmic firing of GABAergic neurons in the medial septum and diagonal bands: an investigation using a complete septohippocampal preparation in vitro. J Neurosci 28(15):4096-4107.
24. Akam T, Oren I, Mantoan L, Ferenczi E, & Kullmann DM (2012) Oscillatory dynamics in the hippocampus support dentate gyrus-CA3 coupling. Nat Neurosci 15(5):763-768.
25. Song I, et al. (2013) Different transporter systems regulate extracellular GABA from vesicular and non-vesicular sources. Front Cell Neurosci 7:23.
26. Turner DA (1984) Conductance transients onto dendritic spines in a segmental cable model of hippocampal neurons. Biophys J 46(1):85-96.
27. Kopell N, Kramer MA, Malerba P, & Whittington MA (2010) Are different rhythms good for different functions? Front Hum Neurosci 4:187.
28. Pavlov I, Savtchenko LP, Kullmann DM, Semyanov A, & Walker MC (2009) Outwardly rectifying tonically active GABAA receptors in pyramidal cells modulate neuronal offset, not gain. J Neurosci 29(48):15341-15350.
29. Zheng K, Scimemi A, & Rusakov DA (2008) Receptor actions of synaptically released glutamate: the role of transporters on the scale from nanometers to microns. Biophys J 95(10):4584-4596.